Received: 16 April 2024 | Accepted: 9 September 2024 | Published online: 25 September 2024

DOI: 10.1002/saj2.20767

Soil Science Society of America Journal

TECHNICAL NOTE

Fundamental Soil Science

Fate of As(V) and Cr(VI) adsorbed on goethite in a mangrove-microcosm experiment

Matheus Sampaio C. Barreto[1] | **Francisco Ruiz**[2] | **Luis C. Colocho Hurtarte**[3,4] | **Tiago Osorio Ferreira**[2] | **Donald L. Sparks**[1]

[1]Department of Plant & Soil Sciences, University of Delaware, Newark, Delaware, USA

[2]Department of Soil Science, "Luiz de Queiroz" College of Agriculture, University of São Paulo, Piracicaba, São Paulo, Brazil

[3]European Synchrotron Radiation Facility, Grenoble, France

[4]Diamond Light Source, Rutherford Appleton Laboratory, Didcot, UK

Correspondence
Matheus Sampaio C. Barreto, Department of Plant & Soil Sciences, University of Delaware, 476 Harker ISE Lab, Newark, DE 19716, USA.
Email: mbarreto@udel.edu

Assigned to Associate Editor Patrick Tomco.

Funding information
National Science Foundation, Grant/Award Number: CHE-1428149; Conselho Nacional de Desenvolvimento Científico e Tecnológico, Grant/Award Number: 305013/2022−0; Engineer Research and Development Center, Grant/Award Number: Contract No. W912HZ-20-2-0041

Abstract

Mangroves provide fundamental ecosystem services; however, the growing impact of human activities has resulted in increased pollution pressure, such as chemical contaminants. The redox processes are major biogeochemical players in the fate of contaminants. We investigate the effects of the redox environment on As(V) and Cr(VI) adsorbed on goethite (i.e., Fe(III)-oxide) over 40 days of incubation in columns containing mangrove soil subjected to seawater saturation cycles. Our spectroscopic data highlighted a less Fe(III)-ordered arrangement on goethite over time; As(V) is strongly bound to goethite, which delayed until 20 days its remobilization and reduction to As(III). After 40 days, the goethite held ~50% of the initial As, but it was 15% as As(III). On the other hand, Cr(VI) was desorbed almost completely in less than 10 days, and the residual Cr ions bound to goethite were almost totally converted to Cr(III). Our study stresses the importance of individual time-dependence in evaluating chemical speciation changes among potential toxic elements in wetland systems, such as mangroves and artificial wetlands designed to water treatment or soil remediation.

1 | INTRODUCTION

Mangroves provide a range of key ecosystem services, including feeding and reproduction habitats for a wide variety of marine and terrestrial species, coastal physical protection, and the storage of large amounts of carbon and nutrients (Alongi, 2018; Barcellos et al., 2019; Costanza et al., 2014; Giri et al., 2011; Kauffman et al., 2018). Nevertheless, the growing impact of rapid industrialization, urbanization, and other human activities (e.g., aquaculture) has increased pollution levels, posing a significant threat to mangrove forests worldwide and making them one of the most endangered ecosystems (Duke et al., 2007; Goldberg et al., 2020). Most of the concerns arising from anthropogenic activities that extensively increased environmental quality deterioration of estuarine systems by the introduction of contaminants (Agoramoorthy et al., 2008; Barcellos et al., 2019; Gabriel et al., 2021; Maurya & Kumari, 2021).

The mobility of these contaminants is closely linked to complex biogeochemical processes, which in mangroves are mostly related to the complexation by organic matter (Lacerda et al., 1991; Öztürk et al., 2021; Tuzen et al., 2009),

adsorption on Fe and Mn oxyhydroxides, silicate minerals, and carbonates, and (co)precipitation with sulfides (Andrade et al., 2012; Pan et al., 2023). Due to the high amounts of organic matter and waterlogging conditions, redox biogeochemical processes are major drivers of the fate of several potentially toxic elements (Borch et al., 2010). For instance, under suboxic or anoxic conditions, Fe(III)-oxyhydroxides can be reduced by biotic and abiotic processes and may mobilize contaminants previously adsorbed (Barreto, Wani, et al., 2024; Wu et al., 2019; C. Yu et al., 2021). Furthermore, arsenic (As), a major threat to human health and flagged as a priority contaminants in soil and water by the US Environmental Protection Agency (USEPA, 1996), can undergo reduction from arsenate (As(V)) to arsenite (As(III)), the latter characterized by a much higher toxicity (Hughes, 2002; Jomova et al., 2011). Contrastingly, chromate (Cr(VI)), which is also highly toxic to animals and plants, may be reduced to the nontoxic Cr(III) (DesMarias & Costa, 2019), which is listed as an essential element for the good health and nutrition of many organisms (Levina & Lay, 2008).

Our previous work described the strong stability of adsorbed As(V) onto ferrihydrite against wide pH variation (Barreto et al., 2023). On the other hand, Cr(VI) was extensively released due to remobilization by pH variation or by competition with 1% artificial seawater concentration (Barreto, Elzinga, Kubicki, et al., 2024). Nevertheless, the impact of the active redox environment of mangrove soils on the in situ reduction of previously adsorbed As(V) and Cr(VI) onto Fe(III)-oxides, as well as their possible remobilization, remains uncertain. In this study, we investigated the effects of the redox environment on As(V) and Cr(VI) previously adsorbed onto goethite. This investigation involved the incubation of samples in columns filled with mangrove soil subjected to daily cycles of seawater saturation and draining. We applied both X-ray photoelectron spectroscopy (XPS) to provide the chemical composition of the mineral surfaces (Krishna & Philip, 2022) and X-ray absorption near edge structure spectroscopy (XANES), as a direct method for determining the speciation of the elements of interest (Barreto, Elzinga, Rouff, et al., 2024; Fendorf et al., 1997; Gomes et al., 2022; Sparks, 2003). Such approaches can offer valuable insights on the mobility of contaminants and their chemical speciation changes resulting from redox processes in mangrove soils.

Core Ideas

- The redox processes are major biogeochemical players in wetlands.
- Goethite surface changes to less-ordered structure in mangrove soils.
- Fast Cr(VI) mobilization in mangrove soils, however, is reduced to Cr(III).
- Slow As(V) release in mangrove soils, however, is reduced to As(III).

2 | MATERIALS AND METHODS

2.1 | Site description, sample collection, and characterization

The soil was collected from a mangrove in Southeast Brazil (19°56′58″ S, 40°59′23″ W, Piraquê-mirim river estuary, Espírito Santo State coastline, Brazil). Stainless steel samplers 50 cm long and 5 cm in diameter were used to collect a mangrove soil core. Sampling was carried out in triplicate to ensure that enough material was collected. The pH (HANNA instruments; model HI991003) and salinity (handheld refractometer RHB82, ranging from 0 to 100 parts per thousand [ppt]) were measured in each borehole, which reached, on average, 7.1 units and 36 ppt, respectively. The soil samples (top 10–20 cm) were taken from the core tubes, which were hermetically sealed in polythene packets, kept under refrigeration (approximately 4°C), and brought to the laboratory at Escola Superior de Agricultura Luiz de Queiroz (ESALQ/USP).

At the laboratory, the soil samples were immediately homogenized in a N_2 atmosphere glovebox. A subsample was used for chemical and particle size distribution analyses according to the methodologies used routinely in the lab (van Raij et al., 2001). The soil contained 23% clay, mainly composed of kaolinite and gibbsite (data not shown), had a pH of 7.4 (0.01 M $CaCl_2$ at a ratio of 1: 2.5 v/v), and an organic C content of 42.5 g kg^{-1} (determined by an elemental LECO CN-2000 analyzer) after carbonate removal. The concentrations of As and Cr naturally present in the soil were determined by performing hotplate aqua regia digestion, followed by analysis with Inductively coupled plasma optical emission spectrometry (Chen & Ma, 2001). The measured concentrations for As and Cr were 50.2 and 39.2 mg kg^{-1}, respectively. These concentrations fall within the range of values previously reported for mangroves in the region (Kumar et al., 2015; Mirlean et al., 2012).

2.2 | Sorption of As(V) and Cr(VI) onto goethite

Goethite (α-FeOOH, "Gt") was purchased from Sigma-Aldrich. The specific surface area, measured by the BET method (N_2 adsorption–desorption isotherms at 77 K), was 19.9 m^2 g^{-1}. An adsorption isotherm experiment was conducted at pH 5 and with 100 mM NaCl (background solution) to estimate the maximum adsorption capacity (Qmax) of As(V) and Cr(VI) on Gt using the Langmuir isotherm model.

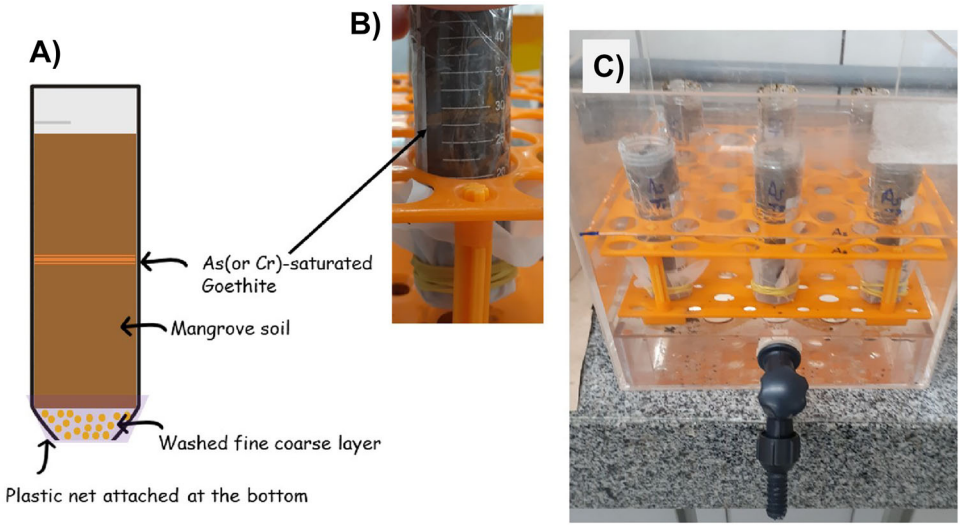

FIGURE 1 (A) A schematic representation of the column of the mangrove-microcosm experiment used for the simulation of redox cycles over contaminated goethite into mangrove soil. (B) The soil column, showing the initial layer of goethite. (C) The water tank where the columns were placed. The tank was gently filled everyday with artificial seawater until it reached the top of the columns. After ~14 h, the solution was removed and the columns were drained. After ~10 h, the tank was refilled for a new cycle of column saturation. The temperature was kept at 22 ± 2°C throughout the incubations and most of the time in the dark to minimize any photochemical reactions.

The Qmax of As(V) was 2210 mg kg^{-1} and for Cr(VI) was 1560 mg kg^{-1}. The detailed experimental method is described elsewhere (Barreto et al., 2020).

The saturation of Gt was performed by weighting 10 g in a 50-mL tube and adding 25 mL of 0.1 M of As(V) (as Na_2HAsO_4) to produce Gt-As(V). After 24 h, the solution pH was adjusted to 5 by the addition of 0.1 M NaOH or 0.1 M HCl and continued to be mixed via stirring for 3 days. After that, the tubes were centrifuged, the supernatant discarded, and the solids washed twice with 40 mL of 70% acetone to eliminate unbound As(V) held in the interstitial water. The residual solids were dried at 45°C for 72 h, ground, and thoroughly homogenized for further use. The same procedure was repeated for Gt-Cr(VI) saturation by using 25 mL of 0.1 M of Cr(VI) (as K_2CrO_4) for saturation.

2.3 | Column experiment

A column consisting of a 50-mL laboratory tube with an open bottom to simulate a soil column was used with a plastic net attached at the column ends (Figure 1). A fine sand was added (4 g) to ensure free water movement and avoid the loss of soil particles. The homogenized soil samples were then packaged up to half of the column length, followed by 1.00 g of As(V) (or Cr(VI)) sorbed Gt, and finally the columns were fully filled with mangrove soil. The position of the sorbed Gt placed in the tube height was recorded. The columns were placed inside a plastic container (~15 L), which was filled with ~8 L of artificial seawater solution (ASTM, 2021) to the top of the column (Figure 1). The daily cycle consisted of ~14 h (overnight) of saturation and ~10 h of draining to simulate the daily tidal frequency observed at the Piraquê-mirim estuary. The solution was collected and reserved for reuse in the new cycle of saturation. The columns were freely drained until a new cycle of saturation began. The temperature was kept at 22 ± 2°C throughout the incubations and most of the time in the dark to minimize any photochemical reactions. This process was repeated throughout the experiment.

We measured the pH and Eh of the solution and harvested two columns for each contaminant (i.e., duplicate) after 10, 20, and 40 days of incubation. The soil columns were then frozen (−20°C), and the Gt was recovered after sawing the column at the Gt position, minimizing any soil/goethite mixture. The recovered Gt was transferred to an anaerobic glovebox (N_2 > 99.5%) for drying and then ground for further analysis. The sample datasets correspond to the initial saturated Gt (i.e., initial Gt + As or Gt + Cr) and those after 10, 20, and 40 days of incubation.

2.4 | XPS and XANES analysis

The initial saturated Gt (before incubation) and composite saturated Gt samples (recovered after incubation) were analyzed by XPS using a K-Alpha X-ray photoelectron spectrometer (Thermo Fisher Scientific) equipped with a monochromatic Al Kα (1486.6 eV) radiation source and a chamber pressure lower than 10^{-8} Pa. High-resolution spectra for Fe, Cr, and As were acquired using a pass energy of 20 eV and a step size of 0.1 eV. The binding energies were referenced to the C1s peak at 284.6 eV for calibration. The XPS results correspond to

an average of 10 independent measurements collected in different regions of each sample. The As 3d region spectra were deconvoluted using high-resolution spectra after Shirley background subtraction by nonlinear least-squares curve-fitting. The As 3d region was analyzed by considering the doublet due to spin-orbit splitting, with a BE difference of 0.68 eV, equal FWHM, and an area ratio between $3d_{5/2}$ and $3d_{3/2}$ contributions of 3:2, using a mixture of Gaussian and Lorentzian functions (70/30) (Burton et al., 2010; Nesbitt et al., 1995). This data processing was done using CasaXPS software.

After XPS data analysis, we observed that the Cr 2p signal was unsuitable for further analysis of oxidation states. Thus, we applied XANES spectroscopy to analyze the Cr-saturated sample. The same composite sample was pressed into a pellet, glued to Kapton tape, and sealed with Ultralene. The Cr X-ray absorption spectra were recorded on the ID21 (Salomé et al., 2013) beamline at the European Synchrotron Radiation Facility (ESRF). The monochromator was calibrated using Cr metal (Cr°) foil. Spectra were collected in fluorescence mode at the Cr K-edge (i.e., E_0 assigned as 5898 eV) and at room temperature using a Si Drift Diode detector (SGX 100 mm^2 SiriusSD silicon drift diode). XANES data were acquired with a dwell time of 0.1 s and a step size of 5 eV from −100 to +120 eV relative to the edge (E_0). Total 10 scans were collected for each sample to improve the signal:noise ratio. The scans obtained for each sample were checked for energy calibration, averaged, the background subtracted, and normalized using the Athena program, an interface to IFEFFIT (Newville, 2001; Ravel & Newville, 2005).

3 | RESULTS AND DISCUSSION

During the experiment, there was a slight decrease in pH from 7.4 to 7 (Figure 2A), close to the value observed in the field. Additionally, the Eh initially was close to 0, decreasing to −78 mV after 10 days, then increasing to ∼+120 eV after 20 and 40 days. These results support an anoxic/suboxic environment in our system (i.e., low oxygen availability) over the incubation time. The total concentration of As and Cr measured by XPS at the surface of Gt showed a different behavior over the incubation period (Figure 2A).

During the first 20 days, the As concentration remained stable, close to 80% of the initial concentration on the Gt surface. This initial decrease may have been due to (1) the pH increase from 5, which the Gt-saturation process was carried; to 7.5, which is the initial pH conditions of the experiment (Figure 2A); and (2) the competition with other anions (e.g., sulfate) and organic acids on the Gt adsorption sites (Barreto et al., 2020). Additionally, as Gt was in contact with seawater solution, other ions, such as Na, Cl, S, and Ca, likely sorbed onto the Gt surface, diluting the As signal from the Gt surface. However, after 40 days, only ∼55% of the initial As concentration remained on the Gt surface (Figure 2A), indicating that desorption increased with time, concomitant to Fe(III) structural changes on the Gt surface. On the other hand, Cr was almost totally released after 10 days, reaching values close to the detection limit (0.1% atomic percentage) after 40 days (Figure 2A). These results support previous studies that highlighted the strong binding of As to Fe-minerals, while Cr appears to have a lower affinity compared to As being desorbed by the high concentration of sulfate present in the artificial seawater (Barreto, Elzinga, Kubicki, et al., 2024).

The high-resolution XPS spectra of the Fe 2p region showed strong peak lines at ∼725.1 eV for $2p_{1/2}$ and ∼711.3 eV for $2p_{3/2}$, regardless of incubation time (Figure 2B). These values and the difference between these lines equal 13.8 eV, confirming Fe^{3+} presence in the Gt surface structure (Grosvenor et al., 2004). However, a slight spectral shoulder at the higher binding energy surface peak for $2p_{1/2}$ and $2p_{3/2}$ appeared after 40 days in both Gt samples with As or Cr (Figure 2B, red arrows).

We believe that the decrease in coordination number of Fe^{3+} ions (i.e., from 6 to 5 or 4; Wilke et al., 2001) and the presence of a new immediate neighbor with lower electronegativity (e.g., SOM-Fe(III) complexes (Bhattacharyya et al., 2022) and/or $Fe_2(SO_4)_3$-precipitated), might decrease the electron density around the ferric ions, consequently demanding more energy to emit a photoelectron peak (Descostes et al., 2000; Fan et al., 2014; Yamashita & Hayes, 2008). The observed change from high- to low-crystallinity of Fe(III) is a common occurrence during Fe(III) reduction in the presence of organic matter and low oxygen availability (Abdala et al., 2020; Queiroz et al., 2022; Roden & Zachara, 1996).

The deconvolution of high-resolution XPS spectra of the As 3d region indicated that As(V) remained as the dominant species after 10 days of incubation. However, 2% of As(III) was observed after 20 days, then its contribution achieved 15% after 40 days of incubation (Figure 3A). The increase in As(III) (Figure 3A) was concomitant with a decrease in the concentration of total As on the Gt surface (Figure 2A) and with changes in Fe(III) arrangement on the Gt surface (Figure 2B).

The affinity of As(V) and As(III) on Fe-oxides depends on the solution pH and composition (Manning et al., 1998). At a pH of 7−8, as observed in our experiment, Dixit and Hering (2003) found that As(III) showed similar or greater adsorption than As(V) on Gt. These authors concluded that As(V) reduction would not increase its mobility, yet the As mobility is closely related to the reductive dissolution of the iron oxyhydroxide, which is supported by other studies (Masscheleyn et al., 1991). For instance, the calculated hydrated ion size of the As(III) species at pH 6.0 was 4.22 Å, and thus smaller than As(V) (5.90 Å) (Zheng et al., 2023), which should favor As(III) adsorption over As(V). We postulate that As(III) competed with adsorbed As(V) for

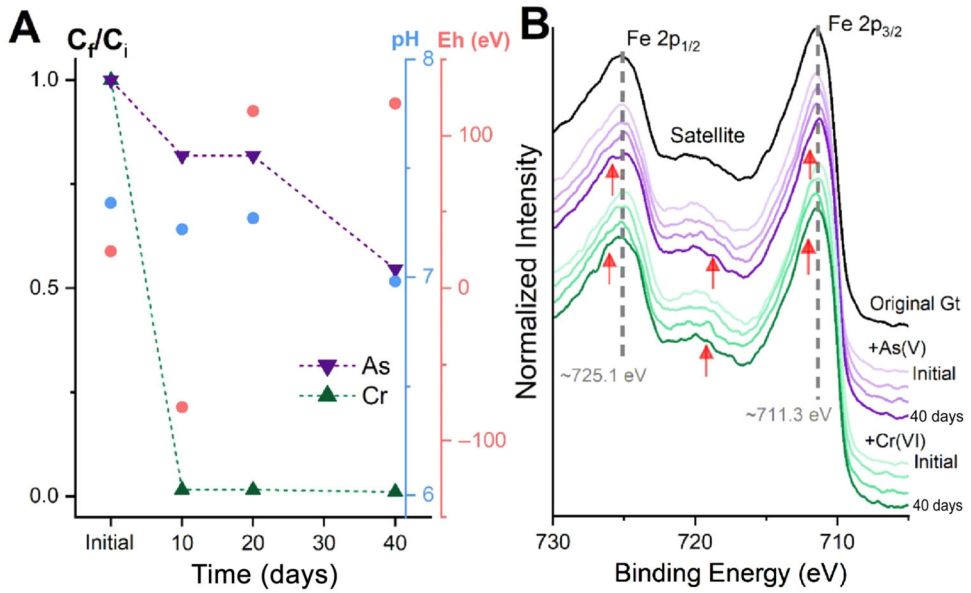

FIGURE 2 (A) Time-dependent change in the atomic percentage (final [C_f]: initial [C_i] concentration ratio) of chromium (Cr, green line and triangles), arsenic (As, purple line and inverted triangles), the pH (blue dots), and Eh (mV, red dots) measured at the beginning and over time. (B) High-resolution XPS spectra of the Fe 2p region of initial Gt (black line), Gt with As(V) (purple lines), and Gt with Cr(VI) (green lines) at initial (i.e., Gt sorbed with As(V) or Cr(VI)) and after 10, 20, and 40 days of incubation. The spectra were normalized to improve clarity. The Fe2p$_{1/2}$ and Fe2p$_{3/2}$ have binding energies of 725.1 and 711.3 eV, respectively, and the difference between these lines is $\Delta = 13.8$ eV. All these values are typical features of Fe(III) species found on the Gt surface. Red arrows highlight spectral disturbances over incubation time.

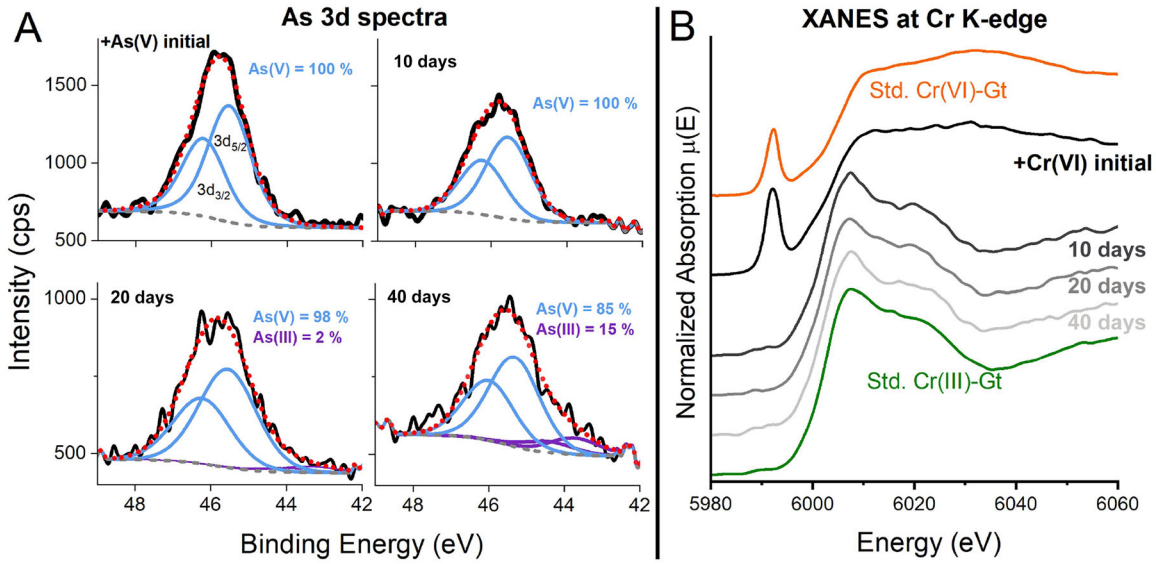

FIGURE 3 (A) High-resolution XPS spectra of the As 3d region of the initial Gt with As(V) and after 10, 20, and 40 days of incubation. The black line shows the experimental raw data, and the gray dashed lines show the Shirley background. As 3d spectra were analyzed by taking into account the doublet due to spin-orbit splitting; thus, the thin lines in blue have peak positions at 46.2 and 45.5 eV related to As 3d$_{3/2}$ and As 3d$_{5/2}$ contributions of As(V) species, respectively. The purple doublets (peak positions: 44.4 and 43.7 eV) are related to As(III) contributions. The total fit is represented by the red dotted line. (B) Normalized X-ray absorption near edge structure (XANES) Cr K-edge spectra of Cr(VI) of the initial Gt with Cr(VI) adsorbed and after 10, 20, and 40 days of incubation. The orange and green lines are reference spectra related to Cr(VI) and Cr(III) adsorbed on Gt.

adsorption sites on the Gt surface, releasing As(V) to the solution. This may explain the relative As(III) increase along with a decrease in As(V) and total As concentrations.

The extensive Cr release in our experiment produced a low Cr signal in the high-resolution XPS spectra of the Cr 2p region (data not shown), which prevented spectra deconvolution. However, XANES spectroscopy provided suitable data on Cr speciation (Figure 3B). The initial Cr on the Gt surface after saturation with dichromate solution was Cr(VI) as expected; however, the residual not adsorbed Cr on Gt after 10, 20, and 40 days was predominately Cr(III) (Figure 3B). The change in Cr oxidation state (i.e., from Cr(VI) to Cr(III), or vice versa) depends on pH (Eary & Rai, 1988), redox potential (Borch et al., 2010; Fruchter et al., 2000), and microbial activity (Shen & Wang, 1993). All these processes and their variations are expected to occur under the dynamic geochemical conditions observed in mangrove soils.

The extensive and fast Cr release observed by XPS (Figure 2A) suggests high remobilization and availability of Cr under mangrove soil conditions. However, Lacerda et al. (1991) pointed out that less than 10% of total Cr is soluble in 0.1 M HCl in mangrove soils and attributed this Cr immobilization to refractory Cr-organic compounds. These Cr compounds were identified in recent studies, which suggests that some bacterial strains drove the production of soluble Cr(III) after Cr(VI) reduction (Dogan et al., 2011; Puzon et al., 2005). Our XANES data confirmed the Cr(VI) reduction and Cr(III) formation (Figure 3B). Thus, we believe that the Cr released from Gt was likely due to Cr(VI) reduction and posterior soluble organo-Cr(III) mobilization.

The residual Cr(III) observed on Gt might undergo adsorption, surface precipitation, or coprecipitation processes (Charlet & Manceau, 1992). In all cases, the pH around 6.5–7.5 observed in mangrove conditions favored the adsorption of Cr(III) hydrolyzed species (e.g., $Cr(OH)^{2+}$, $Cr_2(OH)_4^{2+}$, or $Cr_6(OH_{12})^{6+}$) (Bradl, 2004). Also taking into account the variations on the Gt surface shown in the Fe-XPS data (Figure 2B), some Cr(III) ions might move to inner crystals of Fe-mineral, as Cr(III) may coprecipitate with Fe(III) (Charlet & Manceau, 1992; Pratt et al., 1997).

4 | CONCLUSIONS AND ENVIRONMENTAL IMPLICATIONS

The deposition and accumulation of contaminants in coastal wetlands is a widespread environmental issue. As(V) and Cr(VI) are major toxic elements to plants, animals, and humans and are thus detrimental to the coastal ecosystem's environmental health. However, the complex and dynamic biogeochemistry processes operating in these areas make predictions on the individual fate of these contaminants. In this study, we employed a microcosm incubation approach to simulate the tidal cycles, providing a way to track how mangrove soil biogeochemistry could change As(V) and Cr(VI) adsorbed on goethite, a natural contaminant scavenger.

Our spectroscopic data highlighted that As(V), Cr(VI), and the Fe(III)-mineral surface are dynamic over incubation time. Specifically, the XPS data suggest a slightly less Fe(III)-ordered arrangement on the goethite surface; As(V) is strongly bound to goethite, which delayed its remobilization and reduction to As(III). On the other hand, Cr(VI) was desorbed rapidly, and the residual Cr ions bound to goethite as Cr(III). Overall, we concluded that Cr (VI) mobilization in mangrove soils and sediments can be significant and fast (i.e., in a few days). On the other hand, the slow decrease in total As concentrations over time is followed by the emergence and accumulation of As(III), which is more toxic than As(V).

Collectively, our results enhance our knowledge of the processes controlling the retention and remobilization of As and Cr compounds by Fe-oxides under varying redox conditions typical of mangrove soils. Also, our study stresses the importance of individual time-dependence in evaluating chemical speciation changes. These results discussed here have direct applications to artificial wetlands designed for water treatment or soil remediation (Shutes, 2001), because targeting Cr(VI) seems an efficient alternative since it fast reduction to less toxic species Cr(III) (Jiang et al., 2021). On the other hand, designed for As(V) treatment should have some precaution related to long-term As(III) formation, and likely remobilization, or even released to the environment as volatile As compounds (Lizama et al., 2011; Rahman et al., 2011). Thus, a specific approach (i.e., substrate, plant, and draining–flooding cycles) should be applied to design the artificial wetland depending on the element (or compound) to be remediated (G. Yu et al., 2022).

Our microcosm method applied here could be useful to explore the behavior of other redox-active elements (e.g., U and Sb) in wetlands, and an innovative experimental approach for future studies related to seawater intrusion and waterlog due to sea level rise. Complementary long-term field and laboratory-based studies are required to observe the behavior of contaminants and the primary sorbents, such as Fe-bearing minerals, to improve predictions of the fate of contaminants in mangroves, as well as in other redox-active wetland ecosystems.

AUTHOR CONTRIBUTIONS

Matheus Sampaio C. Barreto: Conceptualization; data curation; formal analysis; investigation; methodology; software; validation; visualization; writing—original draft; writing—review and editing. **Francisco Ruiz**: Conceptualization; formal analysis; investigation; methodology; writing—original draft. **Luis C. Colocho Hurtarte**: Formal analysis; methodology; resources; writing—original draft. **Tiago Osorio Ferreira**: Project administration; resources;

supervision; writing—original draft. **Donald L. Sparks**: Project administration; resources; supervision; validation; writing—original draft.

ACKNOWLEDGMENTS

The authors acknowledge the US Army Engineer Research and Development Center, which provided the partial funding to conduct the research (Contract No. W912HZ-20-2-0041). XPS analysis was performed using an instrument supported with funds from the National Science Foundation, Major Research Instrumentation, under grant No. CHE-1428149 at the Surface Analysis Facility (University of Delaware). Assistance provided by Tienna Deroy is gratefully acknowledged. Tiago Osorio Ferreira thanks the National Council for Scientific and Technology Development (CNPq) for the grant number 305013/2022−0.

CONFLICT OF INTEREST STATEMENT

The authors declare no conflicts of interest.

ORCID

Matheus Sampaio C. Barreto https://orcid.org/0000-0003-1816-3660

Tiago Osorio Ferreira https://orcid.org/0000-0002-4088-7457

REFERENCES

Abdala, D. B., Gatiboni, L. C., Schmitt, D. E., Mumbach, G. L., Dall'Orsoletta, D. J., Bonfada, E. B., & Veiga, M. (2020). Phosphorus speciation and iron mineralogy in an oxisol after 11 years of pig slurry application. *Science of the Total Environment*, *743*, 140487. https://doi.org/10.1016/j.scitotenv.2020.140487

Agoramoorthy, G., Chen, F.-A., & Hsu, M. J. (2008). Threat of heavy metal pollution in halophytic and mangrove plants of Tamil Nadu, India. *Environmental Pollution*, *155*(2), 320–326. https://doi.org/10.1016/j.envpol.2007.11.011

Alongi, D. (2018). Impact of global change on nutrient dynamics in mangrove forests. *Forests*, *9*(10), 596. https://doi.org/10.3390/f9100596

Andrade, R. A., Sanders, C. J., Boaventura, G., & Patchineelam, S. R. (2012). Pyritization of trace metals in mangrove sediments. *Environmental Earth Sciences*, *67*(6), 1757–1762. https://doi.org/10.1007/s12665-012-1620-4

ASTM. (2021). *ASTM D1141-98: Standard specification for substitute ocean water*. https://www.astm.org/d1141-98r21.html

Barcellos, D., Queiroz, H. M., Nóbrega, G. N., de Oliveira Filho, R. L., Santaella, S. T., Otero, X. L., & Ferreira, T. O. (2019). Phosphorus enriched effluents increase eutrophication risks for mangrove systems in northeastern Brazil. *Marine Pollution Bulletin*, *142*, 58–63. https://doi.org/10.1016/J.MARPOLBUL.2019.03.031

Barreto, M. S. C., Elzinga, E. J., & Alleoni, L. R. F. (2020). Hausmannite as potential As(V) filter. Macroscopic and spectroscopic study of As(V) adsorption and desorption by citric acid. *Environmental Pollution*, *262*, 114196. https://doi.org/10.1016/j.envpol.2020.114196

Barreto, M. S. C., Elzinga, E. J., Kubicki, J. D., Sparks, D. L., & Alleoni, L. R. F. (2024). A multi-scale assessment of the impact of salinity on the desorption of chromate from hematite: Sea level rise implications. *Journal of Hazardous Materials*, *465*, 133041. https://doi.org/10.1016/j.jhazmat.2023.133041

Barreto, M. S. C., Elzinga, E. J., Rouff, A. A., Siebecker, M. G., Sparks, D. L., & Alleoni, L. R. F. (2024). Zinc speciation in highly weathered tropical soils affected by large scale vegetable production. *Science of the Total Environment*, *916*, 170223. https://doi.org/10.1016/j.scitotenv.2024.170223

Barreto, M. S. C., Elzinga, E. J., & Sparks, D. L. (2023). The adsorption of arsenate and p-arsanilic acid onto ferrihydrite and subsequent desorption by sulfate and artificial seawater: Future implications of sea level rise. *Environmental Pollution*, *323*, 121302. https://doi.org/10.1016/j.envpol.2023.121302

Barreto, M. S. C., Wani, R. P., Goranov, A. I., Sowers, T. D., Fischel, M., Douglas, T. A., Hatcher, P. G., & Sparks, D. L. (2024). Carbon fate, iron dissolution, and molecular characterization of dissolved organic matter in thawed Yedoma permafrost under varying redox conditions. *Environmental Science & Technology*, *58*(9), 4155–4166. https://doi.org/10.1021/acs.est.3c08219

Bhattacharyya, A., Kukkadapu, R. K., Bowden, M., Pett-Ridge, J., & Nico, P. S. (2022). Fast redox switches lead to rapid transformation of goethite in humid tropical soils: A Mössbauer spectroscopy study. *Soil Science Society of America Journal*, *86*(2), 264–274. https://doi.org/10.1002/saj2.20382

Borch, T., Kretzschmar, R., Skappler, A., Van Cappellen, P., Ginder-Vogel, M., Voegelin, A., & Campbell, K. (2010). Biogeochemical redox processes and their impact on contaminant dynamics. *Environmental Science & Technology*, *44*(1), 15–23. https://doi.org/10.1021/es9026248

Bradl, H. B. (2004). Adsorption of heavy metal ions on soils and soils constituents. *Journal of Colloid & Interface Science*, *277*(1), 1–18. https://doi.org/10.1016/j.jcis.2004.04.005

Burton, E. D., Johnston, S. G., Watling, K., Bush, R. T., Keene, A. F., & Sullivan, L. A. (2010). Arsenic effects and behavior in association with the Fe(II)-catalyzed transformation of schwertmannite. *Environmental Science & Technology*, *44*(6), 2016–2021. https://doi.org/10.1021/es903424h

Charlet, L., & Manceau, A. A. (1992). X-ray absorption spectroscopic study of the sorption of Cr(III) at the oxide-water interface. *Journal of Colloid & Interface Science*, *148*(2), 443–458. https://doi.org/10.1016/0021-9797(92)90182-L

Chen, M., & Ma, L. Q. (2001). Comparison of three aqua regia digestion methods for twenty Florida soils. *Soil Science Society of America Journal*, *65*(2), 491–499. https://doi.org/10.2136/sssaj2001.652491x

Costanza, R., de Groot, R., Sutton, P., van der Ploeg, S., Anderson, S. J., Kubiszewski, I., Farber, S., & Turner, R. K. (2014). Changes in the global value of ecosystem services. *Global Environmental Change*, *26*, 152–158. https://doi.org/10.1016/J.GLOENVCHA.2014.04.002

Descostes, M., Mercier, F., Thromat, N., Beaucaire, C., & Gautier-Soyer, M. (2000). Use of XPS in the determination of chemical environment and oxidation state of iron and sulfur samples: Constitution of a data basis in binding energies for Fe and S reference compounds and applications to the evidence of surface species of an oxidized pyrite in a carbonate medium. *Applied Surface Science*, *165*(4), 288–302. https://doi.org/10.1016/S0169-4332(00)00443-8

DesMarias, T. L., & Costa, M. (2019). Mechanisms of chromium-induced toxicity. *Current Opinion in Toxicology*, *14*, 1–7. https://doi.org/10.1016/j.cotox.2019.05.003

Dixit, S., & Hering, J. G. (2003). Comparison of Arsenic(V) and Arsenic(III) sorption onto iron oxide minerals: Implications for arsenic mobility. *Environmental Science & Technology*, *37*(18), 4182–4189. https://doi.org/10.1021/es030309t

Dogan, N. M., Kantar, C., Gulcan, S., Dodge, C. J., Yilmaz, B. C., & Mazmanci, M. A. (2011). Chromium(VI) bioremoval by Pseudomonas bacteria: Role of microbial exudates for natural attenuation and biotreatment of Cr(VI) contamination. *Environmental Science & Technology*, *45*(6), 2278–2285. https://doi.org/10.1021/es102095t

Duke, N. C., Meynecke, J.-O., Dittmann, S., Ellison, A. M., Anger, K., Berger, U., Cannicci, S., Diele, K., Ewel, K. C., Field, C. D., Koedam, N., Lee, S. Y., Marchand, C., Nordhaus, I., & Dahdouh-Guebas, F. (2007). A world without mangroves? *Science*, *317*(5834), 41–42. https://doi.org/10.1126/science.317.5834.41b

Eary, L. E., & Rai, D. (1988). Chromate removal from aqueous wastes by reduction with ferrous ion. *Environmental Science & Technology*, *22*(8), 972–977. https://doi.org/10.1021/es00173a018

Fan, J.-X., Wang, Y.-J., Liu, C., Wang, L.-H., Yang, K., Zhou, D. M., Li, W., & Sparks, D. L. (2014). Effect of iron oxide reductive dissolution on the transformation and immobilization of arsenic in soils: New insights from X-ray photoelectron and X-ray absorption spectroscopy. *Journal of Hazardous Materials*, *279*, 212–219. https://doi.org/10.1016/j.jhazmat.2014.06.079

Fendorf, S., Eick, M. J., Grossl, P., & Sparks, D. L. (1997). Arsenate and chromate retention mechanisms on goethite. 1. Surface structure. *Environmental Science & Technology*, *31*(2), 315–320. https://doi.org/10.1021/es950653t

Fruchter, J. S., Cole, C. R., Williams, M. D., Vermeul, V. R., Amonette, J. E., Szecsody, J. E., Istok, J. D., & Humphrey, M. D. (2000). Creation of a subsurface permeable treatment zone for aqueous chromate contamination using in situ redox manipulation. *Groundwater Monitoring & Remediation*, *20*(2), 66–77. https://doi.org/10.1111/j.1745-6592.2000.tb00267.x

Gabriel, F. Â., Ferreira, A. D., Queiroz, H. M., Vasconcelos, A. L. S., Ferreira, T. O., & Bernardino, A. F. (2021). Long-term contamination of the Rio Doce estuary as a result of Brazil's largest environmental disaster. *Perspectives in Ecology and Conservation*, *19*(4), 417–428. https://doi.org/10.1016/j.pecon.2021.09.001

Giri, C., Ochieng, E., Tieszen, L. L., Zhu, Z., Singh, A., Loveland, T., Masek, J., & Duke, N. (2011). Status and distribution of mangrove forests of the world using earth observation satellite data. *Global Ecology and Biogeography*, *20*(1), 154–159. https://doi.org/10.1111/j.1466-8238.2010.00584.x

Goldberg, L., Lagomasino, D., Thomas, N., & Fatoyinbo, T. (2020). Global declines in human-driven mangrove loss. *Global Change Biology*, *26*(10), 5844–5855. https://doi.org/10.1111/gcb.15275

Gomes, F. P., Barreto, M. S. C., Amoozegar, A., & Alleoni, L. R. F. (2022). Immobilization of lead by amendments in a mine-waste impacted soil: Assessing Pb retention with desorption kinetic, sequential extraction and XANES spectroscopy. *Science of the Total Environment*, *807*, 150711. https://doi.org/10.1016/j.scitotenv.2021.150711

Grosvenor, A. P., Kobe, B. A., Biesinger, M. C., & McIntyre, N. S. (2004). Investigation of multiplet splitting of Fe 2p XPS spectra and bonding in iron compounds. *Surface and Interface Analysis*, *36*(12), 1564–1574. https://doi.org/10.1002/sia.1984

Hughes, M. F. (2002). Arsenic toxicity and potential mechanisms of action. *Toxicology Letters*, *133*(1), 1–16. https://doi.org/10.1016/S0378-4274(02)00084-X

Jiang, K., Zhang, J., Deng, Z., Barnie, S., Chang, J., Zou, Y., Guan, X., Liu, F., & Chen, H. (2021). Natural attenuation mechanism of hexavalent chromium in a wetland: Zoning characteristics of abiotic and biotic effects. *Environmental Pollution*, *287*, 117639. https://doi.org/10.1016/j.envpol.2021.117639

Jomova, K., Jenisova, Z., Feszterova, M., Baros, S., Liska, J., Hudecova, D., Rhodes, C. J., & Valko, M. (2011). Arsenic: Toxicity, oxidative stress and human disease. *Journal of Applied Toxicology*, *31*(2), 95–107. https://doi.org/10.1002/jat.1649

Kauffman, J. B., Bernardino, A. F., Ferreira, T. O., Giovannoni, L. R., de O Gomes, L. E., Romero, D. J., Jimenez, L. C. Z., & Ruiz, F. (2018). Carbon stocks of mangroves and salt marshes of the Amazon region, Brazil. *Biology Letters*, *14*(9), 20180208. https://doi.org/10.1098/rsbl.2018.0208

Krishna, D. N. G., & Philip, J. (2022). Review on surface-characterization applications of X-ray photoelectron spectroscopy (XPS): Recent developments and challenges. *Applied Surface Science Advances*, *12*, 100332. https://doi.org/10.1016/j.apsadv.2022.100332

Kumar, V., Sinha, A. K., Rodrigues, P. P., Mubiana, V. K., Blust, R., & De Boeck, G. (2015). Linking environmental heavy metal concentrations and salinity gradients with metal accumulation and their effects: A case study in 3 mussel species of Vitória estuary and Espírito Santo bay, Southeast Brazil. *Science of the Total Environment*, *523*, 1–15. https://doi.org/10.1016/j.scitotenv.2015.03.139

Lacerda, L. D., Rezende, C. E., Aragon, G. T., & Ovalle, A. R. (1991). Iron and chromium transport and accumulation in a mangrove ecosystem. *Water, Air, & Soil Pollution*, *57–58*(1), 513–520. https://doi.org/10.1007/BF00282915

Levina, A., & Lay, P. A. (2008). Chemical properties and toxicity of Chromium(III) nutritional supplements. *Chemical Research in Toxicology*, *21*(3), 563–571. https://doi.org/10.1021/tx700385t

Lizama, A. K., Fletcher, T. D., & Sun, G. (2011). Removal processes for arsenic in constructed wetlands. *Chemosphere*, *84*(8), 1032–1043. https://doi.org/10.1016/j.chemosphere.2011.04.022

Manning, B. A., Fendorf, S. E., & Goldberg, S. (1998). Surface structures and stability of Arsenic(III) on goethite: Spectroscopic evidence for inner-sphere complexes. *Environmental Science & Technology*, *32*(16), 2383–2388. https://doi.org/10.1021/es9802201

Masscheleyn, P. H., Delaune, R. D., & Patrick, W. H. (1991). Effect of redox potential and pH on arsenic speciation and solubility in a contaminated soil. *Environmental Science & Technology*, *25*(8), 1414–1419. https://doi.org/10.1021/es00020a008

Maurya, P., & Kumari, R. (2021). Toxic metals distribution, seasonal variations and environmental risk assessment in surficial sediment and mangrove plants (A. marina), Gulf of Kachchh (India). *Journal of Hazardous Materials*, *413*, 125345. https://doi.org/10.1016/j.jhazmat.2021.125345

Mirlean, N., Medeanic, S., Garcia, F. A., Travassos, M. P., & Baisch, P. (2012). Arsenic enrichment in shelf and coastal sediment of the Brazilian subtropics. *Continental Shelf Research*, *35*, 129–136. https://doi.org/10.1016/j.csr.2012.01.006

Nesbitt, H. W., Muir, I. J., & Prarr, A. R. (1995). Oxidation of arsenopyrite by air and air-saturated, distilled water, and implications for mechanism of oxidation. *Geochimica Et Cosmochimica Acta*, *59*(9), 1773–1786. https://doi.org/10.1016/0016-7037(95)00081-A

Newville, M. (2001). IFEFFIT: Interactive XAFS analysis and FEFF fitting. *Journal of Synchrotron Radiation*, *8*(2), 322–324. https://doi.org/10.1107/S0909049500016964

Öztürk, N., Yazar, M., Gündoğdu, A., Duran, C., Şentürk, H. B., & Soylak, M. (2021). Application of cherry laurel seeds activated carbon as a new adsorbent for Cr(VI) removal. *Membrane and Water Treatment*, *12*(1), 11–21. https://doi.org/10.12989/mwt.2021.12.1.011

Pan, F., Xiao, K., Cai, Y., Li, H., Guo, Z., Wang, X., Zheng, Y., Zheng, C., Bostick, B. C., & Michael, H. A. (2023). Integrated effects of bioturbation, warming and sea-level rise on mobility of sulfide and metalloids in sediment porewater of mangrove wetlands. *Water Research*, *233*, 119788. https://doi.org/10.1016/j.watres.2023.119788

Pratt, A. R., Blowes, D. W., & Ptacek, C. J. (1997). Products of chromate reduction on proposed subsurface remediation material. *Environmental Science & Technology*, *31*(9), 2492–2498. https://doi.org/10.1021/es9607897

Puzon, G. J., Roberts, A. G., Kramer, D. M., & Xun, L. (2005). Formation of soluble organo−Chromium(III) complexes after chromate reduction in the presence of cellular organics. *Environmental Science & Technology*, *39*(8), 2811–2817. https://doi.org/10.1021/es048967g

Queiroz, H. M., Ruiz, F., Deng, Y., de Souza, V. S., Jr., Ferreira, A. D., Otero, X. L., de Lima Camêlo, D., Bernardino, A. F., & Ferreira, T. O. (2022). Mine tailings in a redox-active environment: Iron geochemistry and potential environmental consequences. *Science of the Total Environment*, *807*(Pt 3), 151050. https://doi.org/10.1016/j.scitotenv.2021.151050

Rahman, K. Z., Wiessner, A., Kuschk, P., van Afferden, M., Mattusch, J., & Müller, R. A. (2011). Fate and distribution of arsenic in laboratory-scale subsurface horizontal-flow constructed wetlands treating an artificial wastewater. *Ecological Engineering*, *37*(8), 1214–1224. https://doi.org/10.1016/j.ecoleng.2011.02.016

Ravel, B., & Newville, M. (2005). ATHENA, ARTEMIS, HEPHAESTUS: Data analysis for X-ray absorption spectroscopy using IFEFFIT. *Journal of Synchrotron Radiation*, *12*(4), 537–541. https://doi.org/10.1107/S0909049505012719

Roden, E. E., & Zachara, J. M. (1996). Microbial reduction of crystalline Iron(III) oxides: Influence of oxide surface area and potential for cell growth. *Environmental Science & Technology*, *30*(5), 1618–1628. https://doi.org/10.1021/es9506216

Salomé, M., Cotte, M., Baker, R., Barrett, R., Benseny-Cases, N., Berruyer, G., Bugnazet, D., Castillo-Michel, H., Cornu, C., Fayard, B., Gagliardini, E., Hino, R., Morse, J., Papillon, E., Pouyet, E., Rivard, C., Solé, V. A., Susini, J., & Veronesi, G. (2013). The ID21 scanning X-ray microscope at ESRF. *Journal of Physics: Conference Series*, *425*(18), 182004. https://doi.org/10.1088/1742-6596/425/18/182004

Shen, H., & Wang, Y. T. (1993). Characterization of enzymatic reduction of hexavalent chromium by Escherichia coli ATCC 33456. *Applied and Environmental Microbiology*, *59*(11), 3771–3777. https://doi.org/10.1128/aem.59.11.3771-3777.1993

Shutes, R. B. (2001). Artificial wetlands and water quality improvement. *Environment International*, *26*(5–6), 441–447. https://doi.org/10.1016/S0160-4120(01)00025-3

Sparks, D. L. (2003). *Environmental soil chemistry* (2nd ed.). Academic Press.

Tuzen, M., Sarı, A., Mendil, D., Uluozlu, O. D., Soylak, M., & Dogan, M. (2009). Characterization of biosorption process of As(III) on green algae *Ulothrix cylindricum*. *Journal of Hazardous Materials*, *165*(1–3), 566–572. https://doi.org/10.1016/j.jhazmat.2008.10.020

USEPA. (1996). Proposed guidelines for carcinogen risk assessment. *Federal Register*, *61*(79), 17960–18011.

van Raij, B., Andrade, J. C., Cantarella, H., & Quaggio, J. A. (2001). *Análise química para avaliação da fertilidade de solos tropicais*. Instituto Agronômico de Campinas. https://lab.iac.sp.gov.br/Publicacao/Raij_et_al_2001_Metod_Anal_IAC.pdf

Wilke, M., Farges, F., Petit, P.-E., Brown, G. E., & Martin, F. (2001). Oxidation state and coordination of Fe in minerals: An Fe K- XANES spectroscopic study. *American Mineralogist*, *86*(5–6), 714–730. https://doi.org/10.2138/am-2001-5-612

Wu, S., Vymazal, J., & Brix, H. (2019). Critical review: Biogeochemical networking of iron in constructed wetlands for wastewater treatment. *Environmental Science & Technology*, *53*(14), 7930–7944. https://doi.org/10.1021/acs.est.9b00958

Yamashita, T., & Hayes, P. (2008). Analysis of XPS spectra of Fe^{2+} and Fe^{3+} ions in oxide materials. *Applied Surface Science*, *254*(8), 2441–2449. https://doi.org/10.1016/j.apsusc.2007.09.063

Yu, C., Xie, S., Song, Z., Xia, S., & Åström, M. E. (2021). Biogeochemical cycling of iron (hydr-)oxides and its impact on organic carbon turnover in coastal wetlands: A global synthesis and perspective. *Earth-Science Reviews*, *218*, 103658. https://doi.org/10.1016/j.earscirev.2021.103658

Yu, G., Wang, G., Chi, T., Du, C., Wang, J., Li, P., Zhang, Y., Wang, S., Yang, K., Long, Y., & Chen, H. (2022). Enhanced removal of heavy metals and metalloids by constructed wetlands: A review of approaches and mechanisms. *Science of the Total Environment*, *821*, 153516. https://doi.org/10.1016/j.scitotenv.2022.153516

Zheng, Q., Tu, S., Chen, Y., Zhang, H., Hartley, W., Ye, B., Ren, L., Xiong, J., Tan, W., Kappler, A., & Hou, J. (2023). Micropore sites in ferrihydrite are responsible for its higher affinity towards As(III) relative to As(V). *Geochimica Et Cosmochimica Acta*, *348*, 27–40. https://doi.org/10.1016/j.gca.2023.03.007

How to cite this article: Barreto, M. C., Ruiz, F., Hurtarte, L. C. C., Ferreira, T. O., & Sparks, D. L. (2024). Fate of As(V) and Cr(VI) adsorbed on goethite in a mangrove-microcosm experiment. *Soil Science Society of America Journal*, *88*, 2353–2361. https://doi.org/10.1002/saj2.20767